Geophys. J. Int. (2009) **177,** 743–754 doi: 10.1111/j.1365-246X.2008.04076.x

From Devonian extensional collapse to early Eocene continental break-up: an extended transect of the Kejser Franz Joseph Fjord of the East Greenland margin

Max Voss and Wilfried Jokat

Alfred Wegener Institute for Polar and Marine Research, Columbusstrasse, 27568 *Bremerhaven, Germany. E-mail: Max.Voss@rwe.com*

Accepted 2008 December 5. Received 2008 December 5; in original form 2007 June 30

SUMMARY

Seismic investigations along East Greenland's Fjord Region completed during the last decade provide fundamental insights into the region's crustal structure and tectonic history. A summary of models along a transect through the Kejser Franz Joseph Fjord provides a view from the Precambrian Shield to the Eocene oceanic crust. We conclude that a change of rifting geometry from an upper- to a lower-plate-style margin occurred in early Mesozoic times and formed the >350-km-wide rift zone. Despite the demonstrated asymmetry of the northeast Greenland and conjugate Vøring margins, the change of rift geometries and the direction of rift jumps remain debatable. A combined model for productivity and duration of magmatism is proposed for the northeast Greenland fjord region. We suggest that magmatism started slowly at 58.8 ± 3.6 Ma with a production rate of 1.5×10^{-4} km^3 km^{-1} a^{-1}, which is similar to the productivity of onshore upper and lower lava sequences on the Geikie Plateau. A peak of 9.4×10^{-4} km^3 km^{-1} a^{-1} for 0.5 Myr, and a subsequent productivity of $4.4 \pm 0.3 \times 10^{-4}$ km^3 km^{-1} a^{-1} for 2.5 Myr between 53.3 and 50.8 Ma, produced the majority of melt, but break-up did not occur immediately afterwards. Continuous production of melt, similar to the rate of ocean spreading until C22 (∼50 Ma), contributed to massive magmatic underplating until eventual break-up at 50 Ma. The volumes and production rates show similarities to those obtained from a profile off the southeast Greenland margin but with a major difference in a smaller regional spatial extent.

Key words: Continental margins: divergent; Continental tectonics: extensional; Large igneous provinces; Crustal structure; Atlantic Ocean.

1 INTRODUCTION

The northeast Greenland margin opposes the well-explored Norwegian margin across the northern North Atlantic. Margin evolution concepts and rift geometries on the Greenland margin are often assumed to be the same as on its Scandinavian conjugate (e.g. Mosar *et al.* 2002a). A lack of detailed crustal structure models, especially for the post-Devonian to Tertiary parts of the margin, makes this assumption hard to evaluate. Deep seismic experiments in the last decade (Mandler & Jokat 1998; Schlindwein & Jokat 1999; Voss & Jokat 2007; Voss *et al.* 2009) and potential field modelling (Schmidt-Aursch & Jokat 2005b) have provided fundamental data for rift system analysis at the northeast Greenland margin. Schlindwein & Jokat (1999, 2000) proposed a model for the late Caledonian extension, but did not discuss post-Devonian events. In this paper, we summarize and review the extensional structures on a traverse from the Precambrian shield west of the Greenland Caledonides, across the continental sedimentary basins and shelf region, and into the oceanic basin off the Kejser Franz Joseph Fjord (KFJF; Fig. 1). The objective of this study is to provide an overview of the crustal structures formed during tectonic extension that started with Devonian extensional collapse and culminated in early Eocene opening of the North Atlantic. The early Tertiary magmatic episodes, that is, the duration of magmatism based on predicted production rates, will be discussed on this northeast Greenland margin cross-section.

2 GEOLOGICAL BACKGROUND

The Iapetus Ocean closed during continent–continent collision of Baltica and Laurentia in mid-Silurian times (∼425 Ma). The westward subduction of Baltic crust caused extreme crustal thickening in the Caledonian Belt (Torsvik *et al.* 1996). The early stage of post-collision extension and formation of the fault belt (Fig. 1) occurred in middle to late Silurian times, perhaps due to gravitational collapse and pure shear stretching of the lower crust (Andersen & Jamveit 1990; Milnes *et al.* 1997). An alternative model is that the subduction reverted to exhumation (Fossen & Rykkelid 1992; Rey *et al.* 1997) along a pre-existing, west-dipping shear zone (Schlindwein & Jokat 2000). Discrete extensional

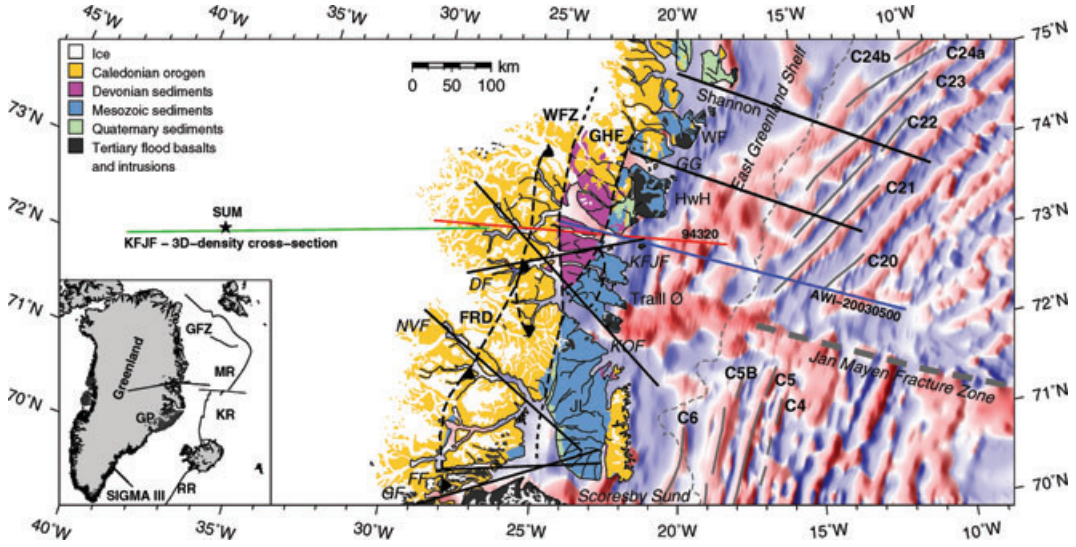

Figure 1. Location of the merged transect from the Precambrian shield west of the Greenland Caledonides into the oceanic basin off the KFJF. Green line marks KFJF—3-D density cross-section after Schmidt-Aursch & Jokat (2005b), profile 94320 (red) after Schlindwein & Jokat (1999) and AWI-20030500 (blue) after Voss & Jokat (2007). Black solid lines mark other seismic profiles. Background shows regional magnetic grid (Verhoef *et al.* 1996) with red regions positive and blue regions negative polarizations. Spreading anomalies are marked with grey lines and labelled with Cxx. Thin black lines represent bathymetric contours after Jakobsson *et al.* (2000). Thick dashed grey line marks the Jan Mayen Fracture Zone. Thin dashed grey line marks smoothed shelf edge (330 m). Onshore geology after Escher & Pulvertaft (1995) (copyright Geological Survey of Denmark and Greenland) and Henriksen *et al.* (2000). Continental extensional detachments and fault zones are marked by black dashed lines. The overview map contains additionally ridges, onshore plateau basalts (dark grey) and locations of the southeast Greenland profile SIGMA III. Abbreviations are DF, Dickson Fjord; FF, Fønsfjord; FRD, Fjord Region Detachment; GF, Gåsefjord; GFZ, Greenland Fracture Zone; GG, Godthåb Gulf; GHF, Gauss Halvø Fault; GP, Geikie Plateau; HwH, Hold with Hope; KFJF, Kejser Franz Joseph Fjord; KOF, Kong Oscar Fjord; KR, Kolbeinsey Ridge; MR, Mohns Ridge; NVF, Nordvestfjord; SUM, Summit station; WF, Wolaston Foreland and WFZ, Western Fault Zone. Scale is valid for 72°N.

phases followed the lithospheric collapse (Dewey 1988; McClay *et al.* 1986) for almost 350 Myr. Extensional detachments (Hartz & Andresen 1995), fault-controlled Devonian basins (Larsen & Bengaard 1991) and syn-extension granitic intrusions along the detachment faults (Hartz & Andresen 1995) testify to the post-Caledonian extension, which ceased in late Devonian to early Carboniferous time. Price *et al.* (1997) suggested minor crustal stretching occurred associated with a Carboniferous rifting event on Traill Ø (Fig. 1), but larger amounts of stretching are suggested for Jameson Land (Larsen 1990; Larsen & Marcussen 1992). Existing seismic refraction data in this area (Fechner 1994; Mandler & Jokat 1998) also show evidence for thinning of the Devonian crust. The most prominent rifting event took place in late Jurassic to early Cretaceous times (Surlyk 1990), when marine sediments were deposited over the Devonian sediments on Jameson Land. North of Kong Oscar Fjord (KOF) these two sequences are juxtaposed (Fig. 1) and separated by the Gauss Halvø Fault (GHF; Schlindwein & Jokat 1999; Peacock *et al.* 2000). Cenozoic magmatism accompanied the final stage of rifting and the opening of the North Atlantic in the early Eocene. Price *et al.* (1997) provide a detailed analysis of the onshore exposures of the Cenozoic rift-related and magmatic rocks. The contrasting rifting histories north and south of the KOF led to the assumption that pre-existing crustal structures had an influence on magmatism (Schlindwein & Jokat 1999). The total amount of volcanic extrusives in the fjord region between KOF and Shannon Island (Fig. 1) is still under debate. The relatively minor tholeiitic and alkaline basalts exposed onshore may either be evidence for weak activity or alternatively represent relics of larger amounts of intrusions which were since eroded (Upton 1988; Larsen *et al.* 1989). Schlindwein & Jokat (1999) and Voss & Jokat (2007) proposed from deep seismic crustal velocity models major melt production in the region between KOF, KFJF and the Godthåb Gulf. Observations of high seismic velocities ($>$7.0 km s^{-1}) in the lower crust are consistently interpreted in this region as magmatic underplating of the northeast Greenland continental crust. The seismic evidence for underplating diminishes rapidly in northern direction (Voss *et al.* 2009). Voss & Jokat (2007) proposed the presence of concealed basaltic extrusives mixed with syn-rift sediments in ∼2–6 km depth within the northeast Greenland shelf region, based on seismic velocities and gravity modelling (Fig. 1). Associated magmatism is related to the opening of the North Atlantic between Greenland and Scandinavia, starting at around 56 Ma from south to north (Larsen 1988). The earliest seafloor spreading is marked by the oldest ocean-spreading anomaly, C24B (∼54 Ma), along the North Atlantic margins (Fig. 1). Voss & Jokat (2007) proposed a delay in break-up in a zone north of the Jan Mayen Fracture Zone (JMFZ), which was locked as a result of long-term extension of the continental crust. Based on the location of the continent ocean boundary (COB) and its obliquity with respect to seafloor spreading anomalies, Voss *et al.* (2009) estimated break-up not earlier than 51.5 $\pm$ 0.2 Ma (C23) and 50.1 $\pm$ 0.3 Ma (C22) off Godthåb Gulf and KFJF, respectively, which is about 3.5 Myr later than that further north. Initially, enhanced oceanic crustal accretion started with half-spreading rates of about 30 cm a^{-1} (Voss *et al.* 2009), and decreased rapidly to 14–17 cm a^{-1} and gave rise to the production of thinner than normal (5–7 km) oceanic crust (White *et al.* 1992). In contrast, the oceanic crust forming off southeast Greenland at the same time is 8–12 km thick (Korenaga *et al.* 2000; Holbrook *et al.* 2001; Hopper *et al.* 2003).

3 CRUSTAL SCALE CHARACTERISTICS OF RIFT EPISODES

A 3-D density model (Schmidt-Aursch & Jokat 2005b) covered parts of the Caledonian hinterland, the fjord region and the Greenland Sea basin up to the Mohns Ridge. Inferences on the structure of the continental crust and sedimentary basins based on six deep seismic profiles (Schlindwein & Jokat 1999; Schmidt-Aursch & Jokat 2005a) over KOF, KFJF, Dickson Fjord (DF), Nordvestfjord (NVF), Fønfjord (FF) and Gåsefjord (GF; Fig. 1). A continent–ocean transition (COT) zone could not be constrained due to the poorly resolved crustal structure, and the COB after Escher & Pulvertaft (1995) was used instead. Constraints for the ocean basin came from Klingelhöfer *et al.* (2000a). The error in extrapolated Moho depths was estimated to ±5 km for the continental domain, and ±3 km in the ocean basin (Schmidt-Aursch & Jokat 2005b). A major uncertainty remains because of poorly known surface geology and westward extent of the Caledonides, hidden beneath the Greenland ice sheet. The newly observed and modelled COT along profile AWI-20030500 (Voss & Jokat 2007) prompt a revised conceptual cross-section through the KFJF (Fig. 1). A composite 1020-km-long traverse is shown in Fig. 2, based on three profiles of seismic refraction data and 3-D density modelling. This traverse provides an excellent basis for re-examining the rifting history and the development of the crustal structural style during post-Caledonian extensional collapse through to the final stage of continental break-up. Multichannel seismic data are not included due to the major focus on deeper crustal structural styles, which is best addressed using wide-angle seismic data. We refer readers to the original studies for details of the velocities, densities, resolutions and uncertainties of the seismic models of the following transects.

(1) The crustal model from the Precambrian shield to the Caledonian mountains (kilometres 0–460) is deduced from a 3-D density cross-section after Schmidt-Aursch & Jokat (2005b). The inland-direction is a prolongation of the offshore seismic transects of the KFJF, and connects to the location of Summit Station (SUM; Dahl-Jensen *et al.* 2003; Fig. 1). The schematic surface topography (Fig. 2) was not included in the density model (Schmidt-Aursch & Jokat 2005b). The profile merges with its eastern neighbour between kilometre 400 at the top and kilometre 460 at the bottom (Fig. 2).

(2) The post-Caledonian structure of the continental crust and sedimentary basins is based on seismic refraction profile 94320 (Fig. 1) in the seaward prolongation of KFJF (Schlindwein & Jokat 1999), between kilometres 400 and 620 (Fig. 2). Intracrustal reflections were located with an accuracy of ±2 km, and the Moho with ±3 km. The transition to the eastern-most profile cuts through kilometres 560 and 620 from top to bottom.

(3) Profile AWI-20030500 covers the COT and the onset of oceanic crust in the Greenland basin. It forms the youngest part of the cross-section from kilometre 560 to the oceanic end at kilometre 1020. The greater number of recording stations and higher ray coverage results in an estimated accuracy of ±0.5 km for upper layers and ±2 km for lower layer boundaries and the Moho (Voss & Jokat 2007). 2-D Bouguer gravity modelling revealed similar densities for the crustal layers, sedimentary basin and upper mantle in the two profiles just described, and it confirms the COT location and high-velocity lower crust.

A review of the typical crustal units (Fig. 2) follows the interpretations of these studies, in combination with the geological maps of Escher & Pulvertaft (1995) and Henriksen *et al.* (2000). The surface geology, faults and large-scale crustal structures are correlated, and the main tectonic events are summarized, in a simplified timescale on Fig. 3.

3.1 Precambrian shield and caledonian orogen

Gravity modelling by Schmidt-Aursch & Jokat (2005b) yielded a thickness of the Proterozoic crust of 35 km (Fig. 2; 0–300 km) with moderate (2.93–3.00 × 10^3 kg m^{-3}) lower crustal densities. This is consistent with the average of other Precambrian shields worldwide (Meissner 1986; Durrheim & Mooney 1994; Christensen & Mooney 1995; Zandt & Ammon 1995). However, Dahl-Jensen *et al.* (2003) inferred a Moho depth of 47 km from receiver function analysis at the SUM, which is about 5 km off the gravity transect near kilometre 125 (Figs 1 and 2). Schmidt-Aursch & Jokat (2005b) showed that using this deeper Moho in the landward prolongation of the KFJF required a density increase from 2.93–3.0 × 10^3 kg m^{-3} between 25 and 35 km to 3.1 × 10^3 and 3.2 × 10^3 kg m^{-3} in the 12 km lower crustal layer, to fit the Bouguer anomaly for the

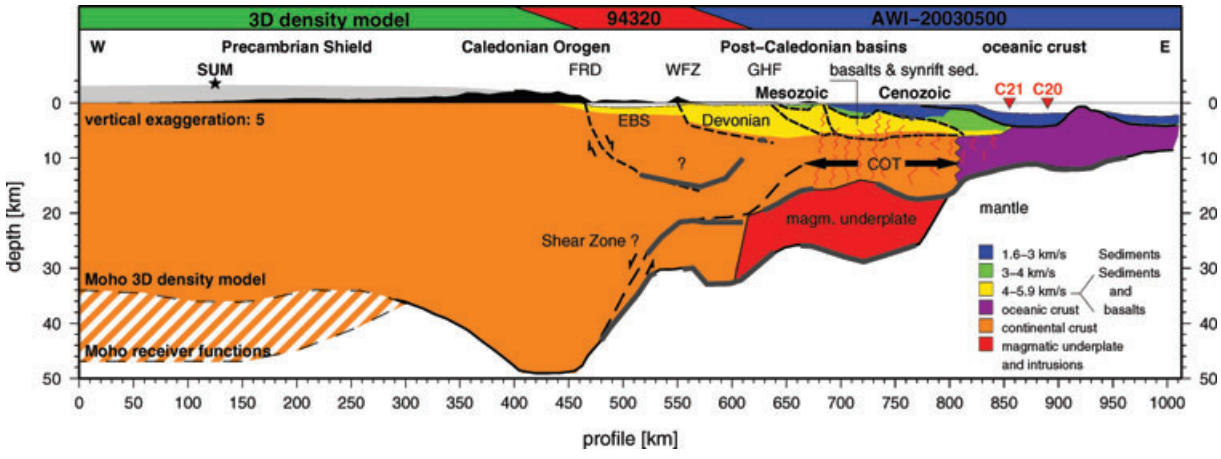

Figure 2. Conceptual crustal model of the merged transects. Coloured bars at top mark extents of single profiles and overlapping regions (see Fig. 1). Colours mark crustal segments and velocity ranges of the sediments and basalts. Grey dashed line marks modelled Moho after 3-D gravity model. Striped region marks high-density lower crustal layer (see the text for details). Solid grey lines mark seismic reflectors. Black short dashed lines mark tectonic structures and/or structural boundaries of basins. Black long dashed line marks possible crustal shear zone. Magnetic spreading anomalies are marked and labelled Cxx. Abbreviations are as in Fig. 1, plus COT, continent–ocean transition; EBS, Eleonore Bay Supergroup sediments; magm., magmatic and sed., sediments.

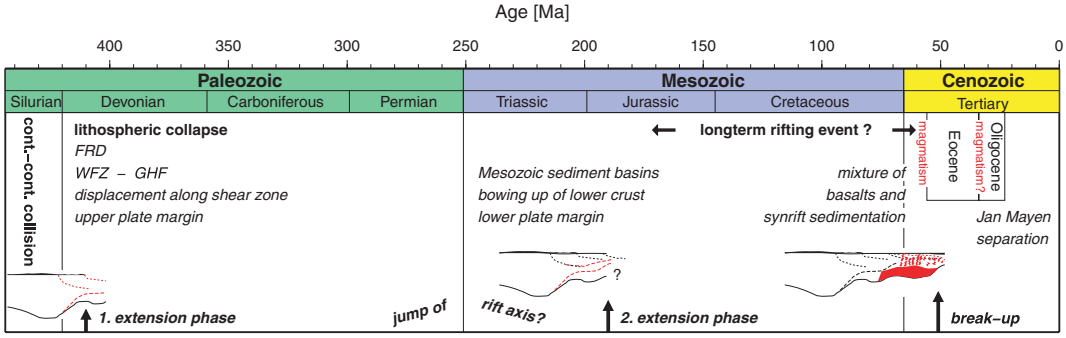

Figure 3. Simplified timescale with main tectonic and magmatic events. A sketch of the transect shows activated structures with red dashed lines. Note the possible jump of the rift axis between Palaeozoic and Mesozoic times. Abbreviations are cont., continent, lith., lithospheric and as in Fig. 2.

Moho (Fig. 2). There is no independent evidence to favour either set of densities, although lower crustal layers with high densities and seismic velocities have been predicted (Durrheim & Mooney 1994) beneath Proterozoic shields. We prefer the simple model associated with the shallower Moho, the lower deep crustal densities and a smoother Moho topography, but without rejecting the other model.

The distinct crustal root (Fig. 2; kilometres 350–500) beneath the Caledonian orogenic belt has a maximum Moho depth of 49 km below sea level, deeper than either of the alternative Moho depths modelled to the west. Clear evidence for this root came from a deep seismic profile in the NVF, and was confirmed by 3-D gravity modelling (Mandler & Jokat 1998; Schmidt-Aursch & Jokat 2005a,b; Fig. 1). The significant Bouguer anomaly low correlates with the highest surface elevations and the crustal root, revealing an overall crustal thickness of 51 km including the caledonian mountains. A crustal root is absent beneath the conjugate Scandinavian Caledonides (Meissner 1986; Kinck *et al.* 1991), where a significant Bouguer anomaly low is instead attributed to lower densities in the mantle (Theilen & Meissner 1979; Bannister *et al.* 1991). Schmidt-Aursch & Jokat (2005b) discuss different orogenic roots and their associated gravity anomalies in detail. An example for an old and preserved crustal root was also found beneath the Proterozoic Torngat Orogen, northeast Canada, between 35 and 38 km thick Archean crust in the west and the Nain Province in the east, which has been preserved for ∼1.8 Gyr (Funck & Louden 1999). A wide Bouguer anomaly low coincides with the ∼50 km deep root, whose formation is suggested either to be the result of a flip in subduction direction (eastward to westward) or, alternatively, from westward underthrusting in a late stage of collision. However, Funck & Louden (1999) attributed the preservation of the crustal root to the absence of post-orogenic heating and ductile reworking, consistent with the lack of post-collisional magmatism. The East Greenland Caledonian crustal root formed in Silurian time (∼425 Ma) during the palaeo-westward subduction of Baltic crust (Torsvik *et al.* 1996). Schlindwein & Jokat (2000) considered gravitational collapse or subduction reverted to exhumation along a west-dipping shear zone. Whether this and/or later heating, for example, due to the Iceland plume thermal anomaly, affected the Caledonian crustal root is presently not understood.

3.2 Post-caledonian basins

3.2.1 Devonian basin

The major east-dipping Fjord Region Detachment (FRD; Fig. 2; Hartz & Andresen 1995; Andresen *et al.* 1998) separates an area unaffected by significant upper crustal extension to the west (Andresen *et al.* 1998), from the Eleonore Bay Supergroup to the east (Fig. 2; 450–550 km). The FRD overlies a steeply westward-dipping Moho at 40–30 km depth. Schlindwein & Jokat (2000) proposed that the FRD terminates at a lower crustal reflector in ∼13 km depth, and that it therefore does not represent a crustal-scale detachment. Those authors proposed that the overthickened post-orogenic Caledonian crust collapsed along a west-dipping shear zone between kilometres 500 and 600 (Fig. 2), which is marked by a prominent lower crustal reflector. They suggest lower crustal displacement along this shear zone, following either a simple shear or a delamination model. The Western Fault Zone (WFZ; Fig. 2) developed during the Devonian subsidence of the thinned crust, and the basin filled with Devonian continental sediments (Larsen & Bengaard 1991; Escher & Pulvertaft 1995). The location of the WFZ at the surface correlates with a Moho high in 30 ± 3 km depth. Schlindwein & Jokat (2000) concluded that this step in the Moho was preserved when the first major rifting phase gradually shifted to the east between late-Devonian and early-Carboniferous times.

3.2.2 Mesozoic basins

The initiation of a second major rifting phase in middle Jurassic times (Surlyk 1990) led to the evolution of Mesozoic sedimentary basins, which lie to the east of the Devonian basin. Middle to upper Jurassic sediments were deposited in fluvial and shallow marine settings (Price *et al.* 1997). A second Moho slope developed during that rifting episode, underlying the GHF (Fig. 2) between the two major sedimentary sequences. The increased seismic velocities of the lower crust in 16–30 km depth (Fig. 2; kilometres 600–680) were interpreted to be a result of (1) the displacement of lower crustal material along the west-dipping shear zone (Schlindwein & Jokat 2000) as described above and (2) Tertiary magmatism (Schlindwein & Jokat 1999; Voss & Jokat 2007). The strong lateral velocity gradient at kilometre 600 can be either a structural boundary between rifted lower continental crust and a pure magmatic underplated body or as the result of an increase in lower crustal intrusions. The correlation between a strong negative magnetic anomaly off the coast (Fig. 1) and the expected magnetization of a lower crustal body led Schlindwein & Jokat (1999) to conclude that the high velocities between kilometres 600 and 680 represent a magmatic underplate.

3.2.3 Continent–ocean transition zone

Rifting persisted until late Cretaceous/early Tertiary times and formed deep-marine clastic wedges of up to 2600 m thickness

exposed in Wolaston Foreland (Surlyk 1978, 1990). Voss & Jokat (2007) suggested that the latest stage of the Cretaceous to Tertiary rifting phase might have been accompanied by magmatism that significantly influenced the style of the COT. Extrusive basalts intercalated with syn-rift sediments form up to 5.4-km-thick layer between kilometres 690 and 810 (Fig. 2). A further conclusion was that a large degree of magmatic intrusions had resulted in an increase in seismic crustal velocities between kilometres 670 and 800 (Fig. 2) in 6–18 km depth (Voss & Jokat 2007) to values (6.6–6.8 km s^{-1}) that are significantly above the global average for extended crust at such depths (Christensen & Mooney 1995). Voss & Jokat (2007) related magnetic anomalies to such intrusions.

A major structure of the COT is a 210 km wide and up to 15-km-thick lower crustal body, interpreted as a solidified magmatic underplate beneath the rifted continental crust (Voss & Jokat 2007). The current transition to mantle rocks occurs beneath the underplate at a depth of 26–28 km, shallowing rapidly eastwards towards the oceanic crust. Schlindwein & Jokat (1999) concluded from the presence of minor exposures of onshore Tertiary plateau basalts on Bontekoe Ø (Fig. 2; kilometre 670), Hold with Hope and Traill Ø (Fig. 1), that the underplate formed contemporaneously with the Tertiary plateau basalts on the Geikie Plateau south of Scoresby Sund (Fig. 1). We cannot preclude the possibility that the thick high-velocity lower crustal body (HVLC) contains fragments of inherited and exhumed Caledonian crust, as in the Norwegian Vøring basin (Gernigon *et al.* 2004). A major difference is, however, the complex magnetic pattern in the northeast Greenland margin associated with major intrusions in the crustal layers. To what extent the HVLC contributes to these magnetic anomalies is open to question, given its depth range of 15–30 km and the unknown level of the Curie temperature (540–570 °C). Schlindwein & Jokat (1999) attributed the large negative magnetic anomaly off the northeast Greenland fjord region (Fig. 1) to the magmatic underplate and expected the demagnetization level to lie below 20 km. We favour, for further consideration, a massive magmatic body and assume the majority of the melt accumulated at the crust-mantle boundary.

3.2.4 Cenozoic basins

Thermal subsidence of the Norwegian-Greenland rift system initiated the deposition of Cenozoic sediments (Fig. 2; kilometres 690–820), which form the top layer of the present East Greenland shelf. The onset of oceanic crust is marked by a deep Cenozoic sedimentary basin (kilometres 810–840) and a steep rise of the Moho to ∼14 km (Voss & Jokat 2007). The accumulation of the magmatic underplate terminated at the time of break-up, and normal accretion of oceanic crust began.

Voss & Jokat (2007) proposed rift propagation from north to south along the Fjord region margin. Break-up was estimated to have occurred last off the KFJF, at close to C22 (∼49.4 Ma) time. Anomaly C21 (∼47.1 Ma) is the first clearly identified magnetic ocean spreading anomaly, at kilometre 850 (Figs 1 and 2). The total thickness of the early Eocene oceanic crust decreases from 7 to 4.8 km (Fig. 2; kilometres 820–980), but with a local maximum of 11.5 km beneath a fragment of the JMFZ (Voss & Jokat 2007; Fig. 2; kilometre 925).

4 RIFT GEOMETRIES

The composite cross-section (Fig. 2) demonstrates the relative dimensions and extents of tectonic and magmatic structures of the COT, the extensional basins and rifted continental crust. Compared to the Precambrian crust and the Caledonian crustal root, a high degree of crustal thinning occurred over a 350-km-wide region from Devonian to Cretaceous times. Post-collision extension involved a significant initial vertical movement of crustal material as seen on the steep eastern flank of the crustal root (Fig. 2; kilometres 460–530). An effective mechanism for crustal thinning and vertical displacement of crustal material is extension along an asymmetric crustal-scale detachment models. The simple shear model (Wernicke 1985) requires a low-angle fault cutting through the entire lithosphere. Extension is accommodated along the fault, and produces related normal faults from upper crustal brittle deformation in the hanging wall. Here, fault-bounded basins develop and fill with clastic sediments. A Moho slope forms where the shear zone offsets. An alternative scenario is the delamination model (Lister *et al.* 1986), which considers a crustal-scale detachment fault, which shears horizontally beneath the brittle/ductile layer boundary of the crust and beneath the Moho. Extension along the shear zone produce equivalent normal faulting at the surface. In either case, asymmetric margins evolve depending on their location relative to the shear zone, as conceptually illustrated in Fig. 4 after Lister *et al.* (1986). The hanging wall is referred to as the upper-plate margin with rocks originally above the shear zone, and with a simple structured basement (Lister *et al.* 1986). Uplift of the continental crust is a response to lateral translation of dense lithospheric material and upwelling of warmer and less denser asthenosphere. Underplating of igneous material at the crust-mantle boundary and normal fault sequences dipping at the surface towards the newly developing ocean are characteristics of an upper-plate margin configuration. The lower-plate margin refers to the footwall, which exposes deeper crustal rocks and hosts wider sedimentary basins. Movement along the major detachment fault and the removal of upper crustal material accompany crustal thinning, subsidence and upward buckling of the lower crust. Characteristics of both upper- and lower-plate margins can be identified along the margin transect in Fig. 2. We propose a rifting model involving a change from an upper- to a lower-plate margin, and which involves subsequent magmatic overprinting.

4.1 Upper-plate margin segment

The main evidence for an upper-plate margin geometry is the inferred westward-dipping lower crustal shear zone (Figs 2 and 5a) with marked reflectivity in 22–40 km depth (Schlindwein & Jokat 2000). Fountain *et al.* (1984) related lower crustal reflectivity to the seismic anisotropy of mylonites along shear zones. The proposed shear zone can be associated with the landward-dipping detachment fault (Lister *et al.* 1986), marked in Fig. 4. Additional structures supporting this model are the major faults, FRD and WFZ, which formed during the first stage of rifting (Fig. 3). Initial vertical displacement of the lower Caledonian crust (Schlindwein & Jokat 2000) is consistent with the early stage of evolution of an upper-plate margin. An eastward prolongation of the proposed shear zone, which cuts through the upper crustal layer (Fig. 5a), can be deduced from the strong lateral upper crustal velocity increase indicated by the dashed line in Fig. 2, from ∼6.3 to ∼6.6 km s^{-1} (Voss & Jokat 2007). Lavier & Manatschal (2006) describe differential crustal motion of up to 10 km vertically accommodated at a ductile shear zone in the thinning mode of the extensional rifting model for non-volcanic margins.

The eastward decrease in exposure of upper crustal material between kilometres 550 and ∼800 in Fig. 2, and the accompanying

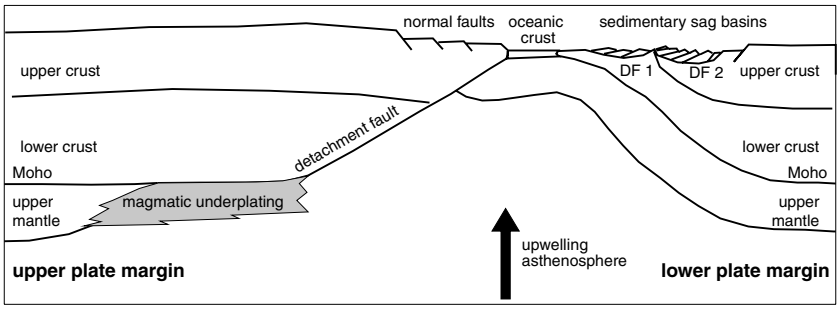

Figure 4. Detachment fault model with complementary asymmetric margin configurations after Lister *et al.* (1986). Upper-plate unstructured, continental uplift due to magmatic underplating. Lower-plate margin has complex structures. Illustration is not to scale. Abbreviations are DF, detachment faults.

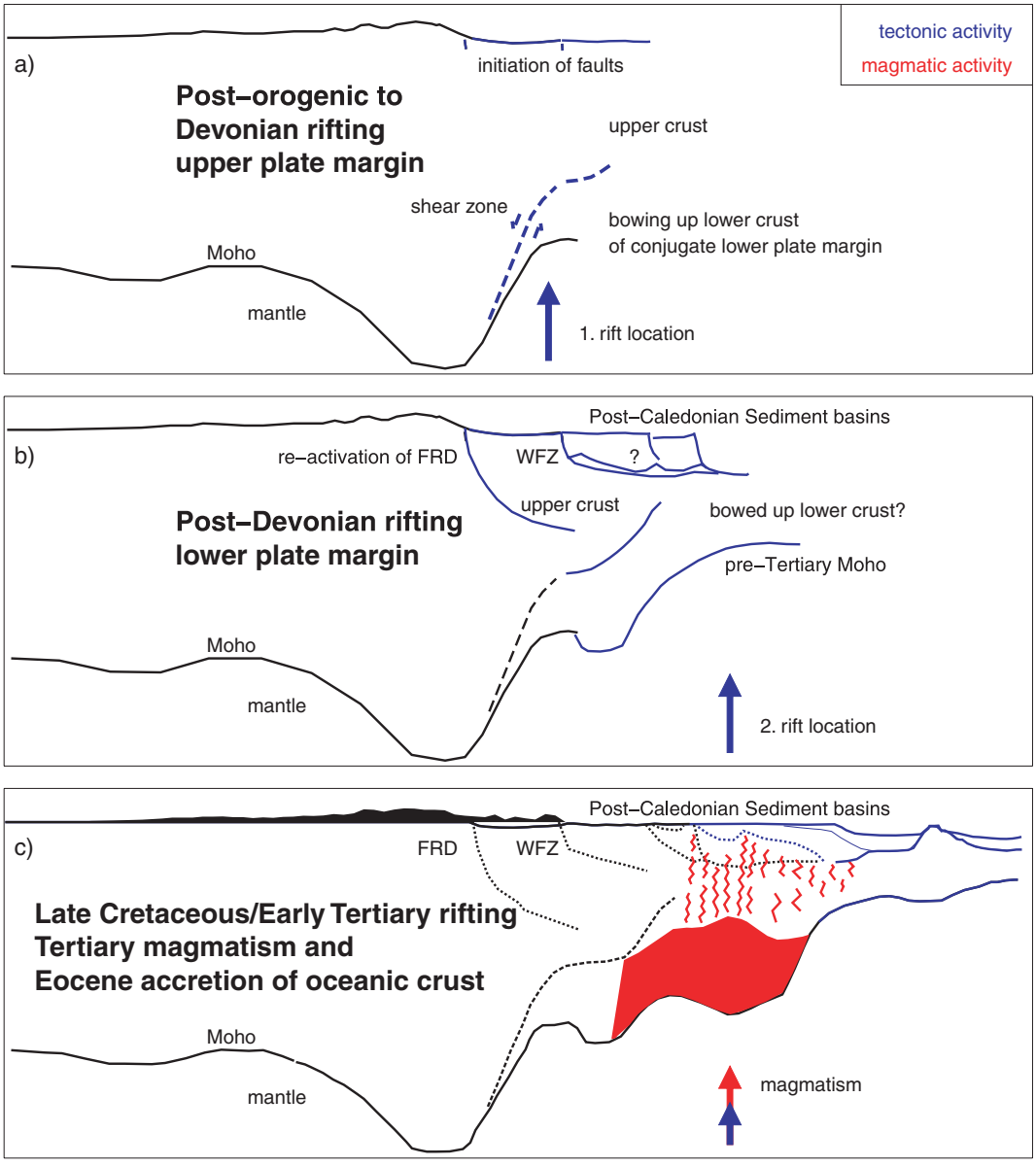

Figure 5. Sketch of the rift geometry and schematic margin evolution. Blue lines mark active faults and structures and red denotes magmatic activity. Arrows (blue and red) mark possible locations of rift and magmatic centres. (a) Post-orogenic to Devonian rifting shows an upper-plate margin configuration. A lower crustal shear zone marks the detachment of the upper and lower plate. Crust of the conjugate lower-plate margin was bowed up. (b) Configuration changed to a lower-plate margin where former detachment faults were re-activated. A shallow pre-Tertiary Moho developed. Upper crust eroded by the eastward drift of the upper plate. (c) Tertiary magmatism attached magmatic underplating and intruded the rifted continental crust. Break-up occurred and initiated accretion of oceanic crust.

evolution of deep extensional basins underlain by large-scale magmatic underplating, do not fit into a full upper-plate margin model. Thus, we suggest a change from the upper-plate margin configuration during the first Devonian/Carboniferous rifting stage to a lower-plate margin configuration in the following rifting stages.

4.2 Lower-plate margin segment

We propose a change to a lower-plate margin with the initiation of the second major phase of rifting further east in the mid-Jurassic (Fig. 3). Supporting evidence comes from Mosar *et al.* (2002a), who inferred as much from the extensional normal faults and the east-dipping FRD, WFZ and GHF. Extension was accommodated by wide-fault blocks (Price *et al.* 1997), whereas, in lower Cretaceous times narrow-fault blocks developed along detachment faults as a consequence of the movement of the eastern (upper) plate. Upper crustal material thinned to some degree during the extensional movement. It is not resolved and thus questionable, whether the post-Caledonian sedimentary basins show eroded half-graben structures at the bottom (Fig. 5b). We suggest from the trend of the isopachs in Voss & Jokat (2007) that the lower crustal material, vertically displaced along the crustal shear zone during the Devonian upper-plate margin stage, bows further upwards during the lower-plate margin stage. To some extent, the lateral velocity increase from ∼6.6 to ∼6.8 km s^{-1} (Voss & Jokat 2007; Fig. 2, marked by dashed line at kilometres 600–650) may mark the transition between the brittle upper crust and ductile lower crustal material in 15–20 km depth, as well as the presence of later magmatic intrusions. A consequence of crustal thinning to less than 10 km was subsidence and the emplacement of syn-rift sediments. Lister *et al.* (1991) describe a similar sequence of crustal thinning and subsidence for Atlantic-type rifted margins based on observations from the US rifted margins. We envision that intrusions into the rifted crust, during Tertiary magmatism at the end of the second rift phase (Fig. 5c) further increased the seismic velocities within the COT, so that originally rifted upper and lower crust cannot be distinguished. There may have been stages of uplift during magmatic underplating, but we neither quantify this nor the accompanying erosion. However, post-magmatic thermal subsidence of ∼3 km can be deduced from the thickness of the post-break-up sedimentary deposits (Fig. 2).

It remains unresolved to what degree the rifted crust is intruded within the COT, and to what extent the high-velocity lower crustal body consists of heavily intruded and stretched continental crust. Sills in continental crust are likely to result in a heterogeneous structural style with enhanced internal seismic reflectivity, but Schlindwein & Jokat (1999) and Voss & Jokat (2007) reported only clear top and bottom reflections of the high-velocity lower crustal body, as shown in Fig. 2.

4.3 Asymmetric rifting of conjugate margins

Torske & Prestvik (1991) proposed a rift-configuration model with an east-dipping main crustal detachment south of the JMFZ and a west-dipping one north of the JMFZ, and suggested an upper-plate style for the East Greenland margin and a lower-plate type Vøring margin. Mosar *et al.* (2002a) also demonstrated asymmetric rifting and the development of upper- versus lower-plate margins for Norway and East Greenland based on cross-sections north and south of the JMFZ. However, the latter authors proposed a lower-plate margin development for East Greenland north of the JMFZ, and did not discuss the influence of magmatism for the latest stage of rifting at either margin. Mjelde *et al.* (2003) favoured a delamination model for the Vøring margin which started as a lower plate in late Cretaceous and early Tertiary times and switched to an upper-plate geometry in response to the arrival of the Icelandic hotspot and a westward jump of the rifting axis. Our model shows a similar jump from an upper- to a lower-plate margin, but suggests the timing of this jump was probably in mid-Jurassic times. The detachment surface is proposed near the top of ductile and heavily intruded lower crust in both models. In light of the uncertainties of the conjugate positions of Kejser Franz Joseph Profile and the Vøring Plateau profile (Voss & Jokat 2007), these two models agree on the evolution of asymmetric margins during the late stages of rifting. They disagree, however, in the timing of tectonic events and styles of rifting in the earlier stages.

5 DURATION AND PRODUCTION RATES OF NORTHEAST GREENLAND MAGMATISM

Estimates of the production rates and the duration of magmatism are very rough because of the large uncertainty in the amount of magma intruded into the lower crust, the proportion of melt that was erupted as basalts and the effect of erosion (Upton 1988; Larsen *et al.* 1989). It should be noted that these rates represent half production rates in units of km^3 per unit length per year (km^3 km^{-1} a^{-1}) based on calculations along only one side of the rift zone.

Table 1 summarizes the total volumes for each part of the rift zone influenced by magmatism and the assumed proportion of melt within the layers. We cannot predict the proportion of basalt and sedimentary rocks at kilometres 690 and 810 (Fig. 2). Thus, we assume it to vary between 0 and 100 per cent with an average of 50 per cent, that is, 210 ± 210 km^3 of basalts. Increasing seismic velocities within the continental crust (kilometres 615–690) and the COT between kilometres 690 and 815 (Fig. 2) could be due to uplifted, dense lower crust, as described above, and/or to intrusions. Therefore, we assume a low variability of 0–20 per cent, averaging 10 per cent, of volcanic intrusions in the rifted continental crust, that is, 210 ± 210 km^3 (Table 1), which is most likely an underestimate. The magmatic underplate (kilometres 600–810) is assumed to consist of entirely magmatic material and has a volume of 1990 km^3 (Table 1). The total volume of basalts, crustal intrusions and magmatic underplating is thus estimated at 2410 ± 420 km^3. An equivalent amount can be assumed from the adjacent profile off the Godthåb Gulf (Voss & Jokat 2007).

Voss *et al.* (2009) proposed a N-to-S propagation of break-up at the northeast Greenland margin, starting at the Greenland Fracture Zone at 54.2 Ma and ending at 50 Ma off the KFJF. We assume, in a first approach, that magmatism was continuous throughout this period and to have had a constant production rate (Table 2). Published half production rates are used for a second calculation and an alternative duration of magmatism is estimated for the region off the KFJF (Table 3).

5.1 Productivity

Voss *et al.* (2009) proposed break-up off the KFJF at 50 Ma near the maximum of the normal polarization of C22. A constant half production rate as high as $5.7 \pm 1.0 \times 10^{-4}$ km^3 km^{-1} a^{-1} must have continued for 4.2 Myr to account for the estimated total magmatism off the KFJF. This corresponds to a half rate of 4.15×10^{-4} km^3

Table 1. Summary of the total magmatic volumes of each part of the rift zone after Voss & Jokat (2007).

	Width (km)	Mean thickness (km)	Total volume (km^3)	Magmatic volume (per cent)
Basalts and sediments	120	3.5	420	210 ± 210 km^3 (0–100)
Transitional/intruded crust	125/200	9.6/10.5	1200/2100	210 ± 210 km^3 (0–20)
Magmatic underplating	210	9.5	1990	1990 km^3 (100)

Notes: Note that the volumes are rough estimates.

Table 2. Half production rates for crustal accretion along the East Greenland margin.

Crustal accretion	Half production rates (km^3 km^{-1} a^{-1})	Crustal thickness (km)	Time interval (Ma)	Reference
NAVP	4.15×10^{-4}		For 3 Myr	Eldholm & Grue (1994)
Mohns Ridge				
0.8 cm a^{-1}	0.3×10^{-4}	∼4.0	0–20	Klingelhöfer *et al.* (2000b)
1.4 cm a^{-1}	0.7×10^{-4}	∼5.0	∼49.4	Voss *et al.* (2009)
2.9 cm a^{-1}	2.9×10^{-4}	∼ 10.0	∼54.2	Voss *et al.* (2009)
SE Greenland				Hopper *et al.* (2003) (SIGMA III)
3.3 cm a^{-1}	$\sim 5.3 \times 10^{-4}$	18.3–13.5	56.0–53.0	
1.95 cm a^{-1}	$\sim 2.3 \times 10^{-4}$	13.5–11.6	53.0–50.8	
1.7 cm a^{-1}	$\sim 1.9 \times 10^{-4}$	11.6–11.2	50.8–50.0	
KFJF	$\sim 5.7 \pm 1.0 \times 10^{-4}$		For 4.2 Myr	This paper

Notes: Locations and oceanic half spreading rates are given in the first column. Volumes for production rates are calculated per 1 km along the rifted margin. Note that the rates are half production rates. Thicknesses of the oceanic crusts and age intervals are shown in the second and third columns. See the text for the time durations for NAVP and KFJF. Abbreviations are hsr, half spreading rate; KFJF, Kejser Franz Joseph Fjord; Myr, million years; NAVP, North Atlantic Volcanic Province and SE, southeast.

km^{-1} a^{-1} (Table 2), which is both lower and sustained for 1.2 Myr less than our estimate. As an alternative to constant production, the latter authors suggested melt production increased during break-up, and then underwent a gradual decrease.

5.2 Duration

The present day Mohns Ridge (Fig. 1) is an ultra-slow spreading ridge (∼0.8 cm a^{-1}; Klingelhöfer *et al.* 2000b) with a mean crustal accretion of 4.0 ± 0.5 km for the period between 20 Ma and present. This corresponds to a magma productivity of just 0.3×10^{-4} km^3 km^{-1} a^{-1} (Table 2). More recent publications (Mosar *et al.* 2002b) proposed initial half spreading rates of 1.3–1.8 cm a^{-1} for the Mohns Ridge and ∼1.5–2.1 cm a^{-1} for the Aegir Ridge. Voss *et al.* (2009) have shown that half spreading rates decreased from an initial maximum of 2.2–2.9 cm a^{-1} between C23 and C24 to about 1.4 ± 0.1 cm a^{-1} until C22 with a corresponding decreasing crustal thickness from ∼10 to 5 km. These values would yield a magma production rate of 0.7–2.9 $\times$ 10^{-4} km^3 km^{-1} a^{-1} (Table 2). Comparable values were found for central–eastern Greenland plateau basalts (Table 3), which range between 1.15 and 1.5 $\times$ 10^{-4} km^3 km^{-1} a^{-1} for the northern Geikie Plateau to $\sim 2.0 \times 10^{-4}$ km^3 km^{-1} a^{-1} for the southern Geikie Plateau and the area between 69°N and Kangerdlugssuaq (Larsen *et al.* 1989). Basalts on Iceland and onshore East Greenland were emplaced at similar rates (Nielsen & Brooks 1981; Table 3).

Assuming a constant production rate of 1.5×10^{-4} km^3 km^{-1} a^{-1}, based on an average of the published values for extrusive basalts, a time interval of 16.1 ± 2.8 Myr would be required to produce the observed 2410 ± 420 km^3 of magmatic material off the KFJF. This, in turn, would place the initiation of magmatism at around 66.1 ± 2.8 Ma, which is older than most estimates. For example, lower plateau basalts were related to a 60–62 Ma igneous phase around Kangerdlugssuaq (Saunders *et al.* 1997) and from drill site 917 off southeast Greenland (Saunders *et al.* 1998). Plateau lavas on Hold with Hope and Wolaston Foreland were also related to the lower series (Upton *et al.* 1995). Price *et al.* (1997) concluded a main period of volcanism in northeast Greenland at 60–54 Ma.

5.3 Poly-productivity model

The two estimates, one with a production rate of $5.7 \pm 1.0 \times 10^{-4}$ km^3 km^{-1} a^{-1} for 4.2 Myr, and one with a period of magmatism of 16.1 ± 2.8 Myr for an average productivity of 1.5×10^{-4} km^3 km^{-1} a^{-1}, represent end-member models. A model with a heterogeneous, rather than constant, productivity rate appears to be most likely. For instance, the eastward increase in thickness of the magmatic underplate may point to an eastward (i.e. later) increase in productivity. Larsen *et al.* (1989) also calculated an increased productivity for the latter episode of NAVP volcanism (Table 3).

We propose a four stage productivity model including production rates derived from onshore plateau basalts and crustal accretion rates of northeastern Greenland. The derived initial magmatism correlates well with the dating of earliest emplaced onshore basalts. Backwards calculation from the time of break-up is necessary to achieve the initial duration. Production rates, duration of the stages and total magmatic volumes are listed in Table 4 and schematically shown in Fig. 6. Half spreading rates for northeast Greenland's oceanic crust and average crustal thicknesses are taken from Voss *et al.* (2009), and the ages of spreading anomalies from Cande & Kent (1995).

Stage IV: The latest stage comprises the magmatic material, which was accreted as oceanic crust from C23 (50.8 Ma) on, but remained beneath the COT zone until the local break-up at 50 Ma. The average half spreading rate for this time interval is proposed as 1.4 ± 0.1 cm a^{-1} and an average crustal accretion of 8 km yields a production rate of $1.1 \pm 0.1 \times 10^{-4}$ km^3 km^{-1} a^{-1}, corresponding to a volume of 88 ± 8 km^3 (Table 4).

Table 3. Half production rates for basaltic provinces.

Basalt provinces	Half production rates ($km^3\ km^{-1}\ a^{-1}$)	Reference
Geikie Plateau	$1.15–2.0 \times 10^{-4}$	Larsen *et al.* (1989)
69°N–Kangerdlugssuaq	$\sim 2.0 \times 10^{-4}$	Larsen *et al.* (1989)
Iceland	$0.6–2.5 \times 10^{-4}$	Nielsen & Brooks (1981)
East Greenland basalts	$0.8–1.0 \times 10^{-4}$	Nielsen & Brooks (1981)
Southeast Greenland	1.12×10^{-4}	Saunders *et al.* (1998)
KFJF	$1.5 \times 10^{-4} \rightarrow 16.1 \pm 2.8$ Myr duration	This paper

Notes: Units are the same as in Table 2. Note that an average of all half production rates is used as an estimate for the KFJF. Abbreviations are as in Table 2.

Table 4. Poly-productivity model for the emplacement of magmatic material off the Kejser Franz Joseph Fjord.

	Productivity ($10^{-4}\ km^3\ km^{-1}\ a^{-1}$)	Duration of magmatism (Myr)	Magmatic volume (km^3)
Stage IV	1.1 ± 0.1	0.8 (50.0–50.8 Ma)	88 ± 8
Stage III	4.4 ± 0.3	2.5 (50.8–53.3 Ma)	1100 ± 75
Stage II	9.4	0.5 (53.3–53.8 Ma)	470 ± 32
Stage I	1.5	5.0 ± 3.6 (53.8–62.4 Ma)	752 ± 535

Notes: See also Fig. 5. Note that the calculation proceeds backwards from the proposed break-up at 50 Ma to reveal the initial duration of magmatism for the given production rate.

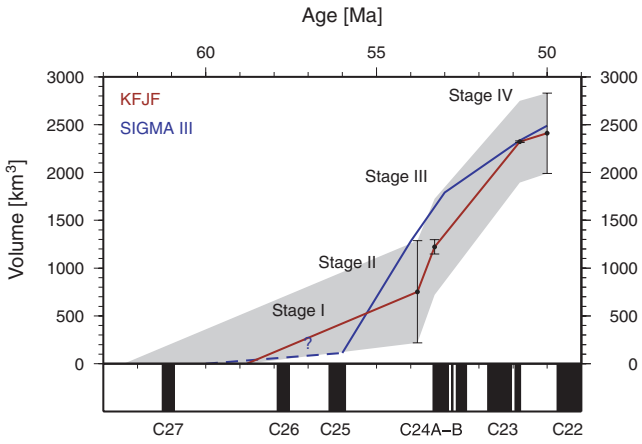

Figure 6. Poly-productivity model for the melt production off the Kejser Franz Joseph Fjord (KFJF) after Table 4. Stages I–IV mark the four different intervals of melt productivity. Duration of magmatism is 8.8 ± 3.6 Ma, initiation is estimated between 55.2 and 62.4 Ma. Red line marks mean values from KFJF, black marks corresponding error bars and grey fill outlines the error region. Production of oceanic crust of the southeast Greenland margin is shown in blue. Note that the question mark and the dashed blue line mark the production of the continental succession, which occurred over 1 Myr within this period. Magnetic spreading anomalies with normal polarization in black are shown as reference after Cande & Kent (1995).

Stage III: An average productivity of $4.4 \pm 0.3\ km^3\ km^{-1}\ a^{-1}$ is deduced from studies of the NAVP after Eldholm & Grue (1994) ($4.15 \times 10^{-4}\ km^3\ km^{-1}\ a^{-1}$) and the lowest limit of the proposed range of the rate for the region off KFJF ($4.7 \times 10^{-4}\ km^3\ km^{-1}\ a^{-1}$; Table 2). This stage has a duration of 2.5 Myr, starting from C23 (50.8 Ma) and lasting until 53.3 Ma (C24B), and produces a magma volume of $1100 \pm 75\ km^3$.

Stage II: A peak of a magma production of $9.4 \times 10^{-4}\ km^3\ km^{-1}\ a^{-1}$ within 0.5 Myr (Eldholm *et al.* 1989; Eldholm & Grue 1994) is used between 53.3 and 53.8 Ma. This results in a contribution of $470 \pm 32\ km^3$ for an equivalent error to that for stage III of 7 per cent.

Stage I: The remaining magmatic volume produced in the initial stage would be $752 \pm 535\ km^3$ (Table 4) deduced from the difference of the total volume along the transect ($2410 \pm 420\ km^3$) and the calculated volumes of the later three stages ($1658 \pm 115\ km^3$). At a production rate of $1.5 \times 10^{-4}\ km^3\ km^{-1}\ a^{-1}$, based on that for the emplacement of the plateau basalts (Tables 3 and 4), the duration of stage I would be 5.0 ± 3.6 Myr.

The model yields a total duration of melt production of 8.8 ± 3.6 Myr (Table 4) and suggests an initiation of magmatism at between 55.2 and 62.4 Ma (Fig. 6). This timing correlates well with the dating of lower plateau basalts (60–62 Ma) around Kangerdlugssuaq (Saunders *et al.* 1997) and the plateau lavas on Hold with Hope and Wolaston Foreland (60–54 Ma; Upton *et al.* 1995; Price *et al.* 1997).

6 DISCUSSION

From the poly-productivity model, we conclude that the maximum magma production at the northeast Greenland margin, that is, off the KFJF and probably also off the Godthåb Gulf, is consistent with the general estimated production rates of extrusives and intrusions for the NAVP. Initiation of magmatism is suggested to have started several million years before the maximum burst of magma in stages II and III (C24B; 53.8 Ma–C23; 50.8 Ma). However, whereas in other regions along the Greenland margin stage III coincides with break-up and emplacement of extensive SDRS basalts, this peak of magmatism off the fjord region preceded break-up there by a few million years. We infer from the change of upper- to lower-plate margin configuration and the associated seaward shift of the rifting centre that the rifted continental crust is only partially weakened, which had an effect on the delayed break-up.

A similar sequence can be discerned at the southeast Greenland margin. Lower lava series on continental crust are dated at 60–60.5 Ma (Saunders *et al.* 1998) from ODP drillhole 917. Hopper *et al.* (2003) proposed a model of magmatism and accretion of oceanic crust along a seismic transect SIGMA III (Fig. 1). These authors estimated an initial half spreading rate of 3.3 cm a^{-1} and identified new igneous crust, which has accreted since 56 Ma. Igneous crustal thickness decreases from 18.3 to 13.5 km within 3 Myr, giving an average productivity of $5.3 \times 10^{-4}\ km^3\ km^{-1}\ a^{-1}$. The productivity decreased further to less than $2.3 \times 10^{-4}\ km^3\ km^{-1}\ a^{-1}$ until 50.8 Ma and $1.9 \times 10^{-4}\ km^3\ km^{-1}\ a^{-1}$ until approximately 50 Ma (Table 2). Continental basalts were proposed to have been emplaced within 1 Myr (at some time between 56 and 61 Ma) with a half production rate of $\sim 1.12 \times 10^{-4}\ km^3$

km^{-1} a^{-1} (Saunders *et al.* 1998; Table 3). The crustal thicknesses, half spreading rates and the emplacement of the continental succession reveal a total volume of approximately 2490 km^3 (Fig. 6). The volume produced off the northeast Greenland margin thus seems equivalent to that at the southeast Greenland margin. The major difference of these two regions is the regional extent of magmatism at the southeast Greenland margin compared to the more localized occurrence of large magmatic volumes off the fjord region (Voss *et al.* 2009). The poly-productivity model with its suggested production rates supports Voss *et al.*'s model of magmatism sourced from one major conduit system in the vicinity of the Icelandic mantle plume and provides a maximum estimate of melt production between 62.4 and 50 Ma for the region off the KFJF, and probably as far as off Godthåb Gulf, which comprises a similar amount of magmatic underplating (Voss & Jokat 2007). Voss *et al.* (2009) proposed alternative models invoking highly intruded continental crust rather than pure magmatic underplating, or a second phase of magmatism linked to the Oligocene separation of the Jan Mayen microcontinent (Fig. 3; Gudlaugsson *et al.* 1988; Upton *et al.* 1995; Price *et al.* 1997). Late Eocene, Oligocene and Miocene magmatism is not included in our model here, although onshore intrusions do indicate ongoing activity (Upton *et al.* 1995; Price *et al.* 1997) associated with the separation of the Jan Mayen and the 30–25 Ma initiation of ocean spreading at the Kolbeinsey Ridge (Larsen 1990; Kodaira *et al.* 1997). The proposed production rates well explain the observed amount of melt off the KFJF and correlate with dated onshore basalts. If the high-velocity lower crustal body has a higher content of rifted continental crust, or if the volume of Oligocene magmatism was comparable to that of the initial early Tertiary event, then the production rates are overestimated and need to be re-evaluated. But the degree of continental crustal content in the high-velocity body and the amount of sill intrusion in upper crustal layers remain debatable and further investigations are necessary. However, slightly lower production rates and a portion of the volume associated with the earliest stage (752 ± 535 km^3) could be related to the Oligocene magmatism.

7 CONCLUSIONS

A crustal transect across the entire East Greenland passive margin is provided, based on deep seismic refraction data and 3-D gravity data modelling. It extends from the Precambrian shield, and through the Caledonian Foreland, to the early Eocene oceanic crust in the prolongation of KFJF. A polyphase rift history and magmatism based on crustal-scale structures can be summarized as follows.

(1) The lithospheric collapse of Caledonian crust initiated the configuration of an upper-plate margin. Devonian rifting corresponds with the displacement of the lower crustal layer along a landward-dipping detachment fault and the initiation of major seaward-dipping faults at the surface. The reflectivity of the deep-seated shear zone can be related to the velocity contrast and/or mylonites along the shear zone.

(2) The geometry changed to a lower-plate margin configuration with the initiation of the second long-term rifting event in Jurrasic times, as suggested by the pattern of velocity increase in the higher crustal levels. The ductile lower crust bowed up, and brittle upper crustal material was eroded during the large-scale extension accompanying the eastward movement of the eastern upper-plate margin. Large low-angle oceanward-dipping faults developed, or were reactivated from the previous rifting event, forming sedimentary basins. An earlier crust-mantle boundary is assumed to be marked by the top reflector of the magmatic underplate at 15–17 km depth.

(3) Margin uplift is assumed with the initiation of early Tertiary magmatism and the emplacement of the magmatic underplate. Basalts erupted either subaerially or in a shallow water setting on uplifted lower crust. Intrusions additionally modified the rearranged and displaced upper and lower crust.

(4) The history of asymmetric rifting for the northeast Greenland lower-plate margin is consistent with the suggestion of an upper-plate margin configuration on the Vøring Plateau in early Tertiary. Our arguments concerning changes of the rift geometry and jumps of the rifting axis during earlier times are, however, at odds with previous studies.

(5) A four stage model is proposed to explain the production of the observed magmatic volume within the rift zone. Magmatism started at 58.8 ± 3.6 Ma, slowly, with the emplacement of onshore plateau basalts. During the peak of magmatism, most of the produced melt accreted along the rift zone but break-up did not occur in the region off the KFJF. Here, ongoing reduced magmatism weakened the highly extended crust. Prior to break-up at C22 (50 Ma), magma remained beneath the transition zone similar to the accretion during seafloor spreading between C23 and C22 elsewhere. The extruded basalts were concealed by the subsequent subsidence of approximately 3–6 km and Cenozoic sedimentation. This sequence of magmatism explains the suggested amount of melt and supports a model of magmatism from one major feeder system into the region off the KFJF and Godthåb Gulf. In the case that our melt volumes are overestimated due to a higher content of continental crust within the high-velocity body or additional Oligocene magmatism associated with the separation of the Jan Mayen Ridge, other models would remain tenable.

ACKNOWLEDGMENTS

We thank M. C. Schmidt-Aursch and V. Schlindwein, who provided the additional digital gravity and velocity models used for the full transect. The manuscript was also greatly improved by comments from V. Schlindwein and Graeme Eagles. The manuscript profited from the thorough reviews of Robert Trumbull and two other anonymous reviewers. All figures were created with GMT (Wessel & Smith 1998).

REFERENCES

Andersen, T.B. & Jamveit, B., 1990. Uplift of deep crust during orogenic extensional collapse: a model based on field studies in the Sogn-Sunnfjord region of western Norway, *Tectonics,* **9,** 1097–1111.

Andresen, A., Hartz, E. & Vold, J., 1998. A late orogenic extensional origin for the infracrustal gneiss domes of the East Greenland Caledonides (72–74°N), *Tectonophysics,* **285,** 353–369.

Bannister, S., Ruud, B. & Husebye, E.S., 1991. Tomographic estimates of sub-Moho seismic velocities in Fennoscandia and strucutral implications, *Tectonophysics,* **189,** 37–53.

Cande, S.C. & Kent, G.M., 1995. Revised calibration of the geomagnetic polarity timescale for the Late Cretaceous and Cenozoic, *J. geophys. Res.,* **100,** 9761–9788.

Christensen, N.I. & Mooney, W.D., 1995. Seismic velocity structure and composition of the continental crust: a global view, *J. geophys. Res.,* **100,** 9761–9788.

Dahl-Jensen, T. *et al*., 2003. Depth to Moho in Greenland: receiver-function analysis suggests two Proterozoic blocks in Greenland, *Earth planet. Sci. Lett.,* **205,** 379–393.

Dewey, J.F., 1988. Extensional collapse of orogens, *Tectonics,* **7,** 1123–1139.

Durrheim, R. & Mooney, W., 1994. Evolution of the Precambrian lithosphere: seismological and geochemical constraints, *J. geophys. Res.,* **99,** 15 359–15 374.

Eldholm, O. & Grue, K., 1994. North Atlantic volcanic margins: dimensions and production rates, *J. geophys. Res.,* **99,** 2955–2968.

Eldholm, O., Thiede, J. & Taylor, E., 1989. Evolution of the Vøring volcanic margin, *Proc. Ocean Drill. Prog. Sci. Results,* **104,** 1033–1065.

Escher, J. & Pulvertaft, T., 1995. Geological Map of Greenland, 1:2 500 000, *Geological Survey of Greenland*.

Fechner, N., 1994. Detailed refraction seismic investigations in the inner Scoresby Sund/East Greenland. *Reports on Polar and Marine Research,* Vol. 143, pp. 1–196, Alfred Wegener Institute of Polar and Marine Research, Bremerhaven.

Fossen, H. & Rykkelid, E., 1992. Postcollisional extension of the Caledonian orogen in Scandinavia: structural expressions and tectonic significance, *Geology,* **20,** 737–740.

Fountain, D.M., Hurich, C.A. & Smithson, S.B., 1984. Seismic reflectivity of mylonite zones in the crust, *Geology,* **12,** 195–198.

Funck, T. & Louden, K.E., 1999. Wide-angle seismic transect across the Torngat Orogen, northern Labrador: evidence for Proterozoic crustal root, *J. geophys. Res.,* **104,** 7463–7480.

Gernigon, L., Ringenbach, J.C., Planke, S. & Le Gall, B., 2004. Deep structures and breakup along volcanic rifted margins: insights from integrated studies along the outer Vøring Basin (Norway), *Mar. Petrol. Geol.,* **21,** 363–372.

Gudlaugsson, S.T., Gunnarson, K., Sand, M. & Skogseid, J., 1988. Tectonic and volcanic events at the Jan Mayen Ridge microcontinent. in *Early Tertiary Volcanism and the Opening of the NE Atlantic,* pp. 85–93, eds Morton, A.C., Parson, L.M., Geological Soc. Special Publ., No. 39, London.

Hartz, E. & Andresen, A., 1995. Caledonian sole thrust of central East Greenland: a crustal-scale Devonian extensional detachment? *Geology,* **23,** 637–640.

Henriksen, N., Higgins, A., Kalsbeek, F. & Pulvertaft, T., 2000. Greenland from Archaean to Quarternary; descriptive text to the geological map of Greenland, 1: 2 500 000, *Geol. Greenland Surv. Bull.,* **185,** 1–93.

Holbrook, W.S. *et al*., 2001. Mantle thermal structure and active upwelling during continentalbreakup in the North Atlantic, *Earth planet. Sci. Lett.,* **190,** 251–266.

Hopper, J.R. *et al*., 2003. Structure of the SE Greenland margin from seismic reflection and refraction data: implications for nascent spreading center subsidence and asymmetric crustal accretion during North Atlantic opening, *J. geophys. Res.,* **108,** 2269–2291.

Jakobsson, M., Cherkis, N.Z., Woodward, J., Macnab, R. & Coakley, B., 2000. New grid of Arctic bathymetry aids scientists and mapmakers, *EOS, Trans. Am. geophys. Un.,* **81**(9), p. 89, 93, 96.

Kinck, J.J., Husebye, E.S. & Lund, C.E., 1991. The South Scandinavian crust: structural complexities from seismic reflection and refraction profiling, *Tectonophysics,* **189,** 117–133.

Klingelhöfer, F., Géli, L., Matias, L., Steinsland, N. & Mohr, J., 2000a. Crustal structure of a super-slow spreading centre: a seismic refraction study of Mohns Ridge, 72°N, *Geophys. J. Int.,* **141,** 509–526.

Klingelhöfer, F., Géli, L. & White, R.S., 2000b. Geophysical and geochemical constraints on crustal accretion at the very-slow spreading Mohns Ridge, *Geophys. Res. Lett.,* **27,** 1547–1550.

Kodaira, S., Mjelde, R., Gunnarson, K., Shiobara, H. & Shimamura, H., 1997. Crustal structure of the Kolbeinsey Ridge, North Atlantic, obtained by use of ocean bottom seismographs, *J. geophys. Res.,* **102,** 3131–3151.

Korenaga, J., Holbrook, W.S., Kent, G.M., Kelemen, P.B., Detrick, R.S., Larsen, H.C., Hopper, J.R. & Dahl-Jensen, T., 2000. Crustal structure of the southeast Greenland margin from joint refraction and reflection seismic tomography, *J. geophys. Res.,* **105,** 21 591–21 614.

Larsen, H.C., 1988. A multiple and propagating rift model for the NE Atlantic. In *Early Tertiary Volcanism and the Opening of the NE Atlantic,* pp. 157–158, eds Morton, A.C., Parson, L.M., Geological Society Special Publication.

Larsen, H.C., 1990. The East Greenland Shelf, in Grantz, A., Johnson, L. & Sweeney, J.F., eds, *The Geology of North America,* pp. 185–210, Geological Society of America, Boulder, Colo.

Larsen, P.H. & Bengaard, H.J., 1991. Devonian basin initiation in East Greenland: a result of sinistral wrench faulting and Caledonian extensional collapse, *J. geol. Soc. Lond.,* **148,** 355–368.

Larsen, H.C. & Marcussen, C., 1992. Sill-intrusion, flood basalt emplacement and deep crustal structure of the Scoresby Sund region, east Greenland. in *Magmatism and the Causes of Continental Break-up,* pp. 365–386, eds Storey, B.C., Alabaster, T., Pankhurst, R.J., Geological Society Special Publication.

Larsen, L.M., Watt, W.S. & Watt, M., 1989. Geology and petrology of the Lower Tertiary plateau basalts of the Scoresby Sund region, East Greenland, *Bull. Grønlands geol. Unders.,* **157,** 1–164.

Lavier, L.L. & Manatschal, G., 2006. A mechanism to thin the continental lithosphere at magma-poor margins, *Nature,* **440,** 324–328.

Lister, G.S., Etheridge, M.A. & Symonds, P.A., 1986. Detachment faulting and the evolution of passive continental margins, *Geology,* **14,** 246–250.

Lister, G.S., Etheridge, M.A. & Symonds, P.A., 1991. Detachment models for the formation of pssive continental margins, *Tectonics,* **10,** 1038–1064.

McClay, K.R., Norton, M.G., Coney, P. & Davis, G.H., 1986. Collapse of the Caledonian orogen and the Old Red Sandstone, *Nature,* **323,** 147–149.

Mandler, H. & Jokat, W., 1998. The crustal structure of central east Greenland: results from combined land-sea seismic refraction experiments, *Geophys. J. Int.,* **135,** 63–76.

Meissner, R., 1986. The continental crust—a geophysical approach, *Int. Geophys. Ser.,* **34**, 426.

Milnes, A.G., Wennberg, O.P., Skår, Ø. & Koester, A.G., 1997. Contraction, extension and timing in the South Norwegian Caledonides: the Sognefjord transect, in *Orogeny Through Time,* pp. 123–148, eds Burg, J.-P., Ford, M., Geological Society Special Publication.

Mjelde, R., Shimamura, H., Kananzawa, T., Kodaira, S., Raum, T. & Shiobara, H., 2003. Crustal lineaments, distribution of lower crustal intrusives and structural evolution of the Voering Margin, NE Atlantic; new insights from wide-angle seismic models, *Tectonophysics,* **369,** 199–218.

Mosar, J., Eide, E.A., Osmundsen, P.T., Sommaruga, A. & Torsvik, T.H., 2002a. Greenland-Norway separation: a geodynamic model for the North Atlantic, *Norwegian J. Geol.,* **82,** 281–298.

Mosar, J., Lewis, G. & Torsvik, T.H., 2002b. North Atlantic sea-floor spreading rates: implications for the Tertiary development of inversion structures of the Norwegian-Greenland Sea, *J. geol. Soc. Lond.,* **159,** 503–515.

Nielsen, T.F.D. & Brooks, C.K., 1981. The East Greenland rifted continental margin: an examination of the costal flexure, *J. geol. Soc. Lond.,* **138,** 559–568.

Peacock, D.C.P., Price, S.P., Whitham, A.G. & Pickles, C.S., 2000. The World's biggest relay ramp: Hold with Hope, NE Greenland, *J. Struct. Geol.,* **22,** 843–850.

Price, S., Brodie, J., Whitham, A. & Kent, R., 1997. Mid-Tertiary rifting and magmatism in the Traill Ø region, East Greenland, *J. geol. Soc. Lond.,* **154,** 419–434.

Rey, P., Burg, J.-P. & Casey, M., 1997. The Scandinavian Caledonides and their relationship to the Variscan belt. in *Orogeny Through Time,* pp. 179–200, eds Burg, J.-P., Ford, M., Geological Society Special Publication.

Saunders, A.D., Fitton, J.G., Kerr, A.C., Norry, M.J. & Kent, R.W., 1997. The North Atlantic Igneous Province, in *Large Igneous Provinces,* pp. 45–94, eds Mahoney, J.J., Coffin, M.F., American Geophysical Union Monograph.

Saunders, A.D., Larsen, H.C. & Wise, S.W.J., 1998. Proceedings of the Ocean drilling Program, Scientific Results, Vol. 152, *Ocean Drilling Program, College Station,* TX.

Schlindwein, V. & Jokat, W., 1999. Structure and evolution of the continental crust of northern east Greenland from integrated geophysical studies, *J. geophys. Res.,* **104,** 15 227–15 245.

Schlindwein, V. & Jokat, W., 2000. Post-collisional extension of the East Greenland Caledonides: a geophysical perspective, *Geophys. J. Int.,* **140,** 559–567.

Schmidt-Aursch, M.C. & Jokat, W., 2005a. The crustal structure of central East Greenland-I: from the Caledonian orogen to the Tertiary igneous province, *Geophys. J. Int.,* **160,** 736–752.

Schmidt-Aursch, M.C. & Jokat, W., 2005b. The crustal structure of central East Greenland-II: from the Precambrian shield to the recent mid-oceanic ridges, *Geophys. J. Int.,* **160,** 753–760.

Surlyk, F., 1978. Jurassic basin evolution of East Greenland, *Nature,* **274,** 311–327.

Surlyk, F., 1990. Timing, style and sedimentary evolution of Late Palaeozoic-Mesozoic extensional basins of East Greenland. in *Tectonic Events Responsible for Britain's Oil and Gas Reserves,* pp. 107–125, eds Hardman, R.F.P., Brooks, J., Geological Society Special Publication.

Theilen, F. & Meissner, R., 1979. A comparison of crustal and upper mantle features in Fennoscandia and the Rhenish Shield, two areas of recent uplift, *Tectonophysics,* **61,** 227–242.

Torske, T. & Prestvik, T., 1991. Mesozoic detachment faulting between Greenland and Norway: inferences from Jan Mayen fracture zone system and associated alkalic volcanic rocks, *Geology,* **19,** 481–484.

Torsvik, T.H., Smethurst, M.A., Meert, J.G., Van Der Voo, R., McKerrow, W.S., Brasier, M.D., Sturt, B.A. & Walderhaug, H.J., 1996. Continental break-up and collision in the Neoproterozoic and Palaeozoic—a tale of Baltica and Laurentia, *Earth-Sci. Rev.,* **40,** 229–258.

Upton, B.G.J., 1988. History of Tertiary igneous activity in the N Atlantic borderlands, *Geol. Soc. Spec. Publ. Lond.,* **39,** 429–453.

Upton, B.G.J., Emeleus, C.H., Rex, D.C. & Thirlwall, M.F., 1995. Early Tertiary magmatism in northeast Greenland, *J. geol. Soc. Lond.,* **152,** 959–964.

Verhoef, J., Macnab, W.R., Arkani-Hamed, R. & Team, J.M.o.t.P., 1996. Magnetic anomalies of the Arctic and North Atlantic Oceans and adjacent land areas; Open File 3125, *Geological Survey of Canada*.

Voss, M. & Jokat, W., 2007. Continent—ocean transition and voluminous magmatic underplating derived from P-wave velocity modelling of the East Greenland continental margin, *Geophys. J. Int.,* **170,** 580–604.

Voss, M., Schmidt-Aursch, M. & Jokat, W., 2009. Variations in magmatic processes along the East Greenland volcanic margin, *Geophys. J. Int.,* doi:10.1111/j.1365-246X.2009.04077.x.

Wernicke, B.P., 1985. Uniform-sense normal simple shear of the continental lithosphere, *Can. J. Earth Sci.,* **22,** 108–125.

Wessel, P. & Smith, W.H.F., 1998. New, improved version of generic mapping tools released, *EOS, Trans. Am. geophys. Un.,* **79,** pp. 579.

White, R.S., McKenzie, D. & O'Nions, R.K., 1992. Oceanic crustal thickness from seismic measurements and rare earth element inversions, *J. geophys. Res.,* **97,** 19 683–19 715.

Zandt, G. & Ammon, C., 1995. Continental crust composition constrained by measurements of crustal Poisson's ratio, *Nature,* **374,** 152–154.